

# New LRFD-based prestressed concrete bulb-tee girders in Colorado

Yail J. Kim and Thushara Siriwardanage

- This paper proposes a new precast concrete bulb-tee girder series for the Colorado Department of Transportation that meets the American Association of State Highway and Transportation Officials' *AASHTO LRFD Bridge Design Specifications*.
- The proposed girder series was developed using the existing Colorado girder series BT618 as the baseline.
- Using bridge software for modeling and analysis, a prototype girder series and a proposed new girder series were studied to optimize the girder section and properties.

**T**ransportation agencies are interested in bridge structures that can be built rapidly at affordably. Prestressed concrete bulb-tee girders have been used for decades in the United States and offer significant structural and economic advantages (such as long spans, controlled cracking behavior, durability, and improved serviceability) compared with reinforced concrete girders. Precast concrete members enable a superior bridge system because they are produced in a controlled plant environment with high quality control and quality assurance. Cost savings are manifested in the employment of precast concrete bridge girders through reusable forms, reduced on-site construction time, and minimal traffic disruption.

Precast concrete bulb-tee girders are ideal structural members for short- and medium-span bridges. They are durable and can be erected without difficulty. According to the "National Bridge Inventory" at the time of writing, there are 2443 prestressed concrete bridges in Colorado.<sup>1</sup> Because the life span of constructed bridges is expected to be at least 75 years, adequate selection of girder types has paramount importance in highway infrastructure. There has been, however, a lack of standardization of prestressed concrete girder configurations. For instance, the web thickness of the American Association of State Highway Transportation Officials (AASHTO) girder family varies from 6 to 8 in. (152.4 to 203.2 mm), whereas that of the AASHTO/PCI girders is consistently 6 in. Some states, for example Washington (Series 14) and Colorado (G72), use a shallow web thickness of 5 in. (127 mm). It is important to note that concrete casting

PCI Journal (ISSN 0887-9672) V. 65, No. 3, May–June 2020.

PCI Journal is published bimonthly by the Precast/Prestressed Concrete Institute, 8770 W. Bryn Mawr Ave., Suite 1150, Chicago, IL 60631.

Copyright © 2020, Precast/Prestressed Concrete Institute. The Precast/Prestressed Concrete Institute is not responsible for statements made by authors of papers in PCI Journal. Original manuscripts and discussion on published papers are accepted on review in accordance with the Precast/Prestressed Concrete Institute's peer-review process. No payment is offered.

should not have any problem when determining the size of a girder web.

Several state departments of transportation (DOTs), such as Nebraska, Washington, Florida, and Indiana, initiated a plan to replace the traditional AASHTO precast concrete girders, either in whole or in part, to meet their own needs for reduced costs with improved structural efficiency.<sup>2</sup> Given that the developed girder sections were not significantly different from the AASHTO sections (which is not a concern when producing girders), there was no reason not to use their own girder families whose performance exceeded that of the conventional AASHTO girder family. Colorado had bulb-tee girders that performed very well (for example, G54 and G68 in the 1960s). Currently Colorado uses BT618 girders, which were developed in the 1990s; however, they are technically outdated because they were designed per the *AASHTO Standard Specifications for Highway Bridges*,<sup>3</sup> which most DOTs do not reference anymore. For instance, Colorado adopted load- and resistance-factor design (LRFD) in 2000. Accordingly, the structural efficiency and performance of these outdated girders may not be best achieved when the *AASHTO LRFD Bridge Design Specifications*<sup>4</sup> are implemented. A new set of bulb-tee girders is therefore required in Colorado to maximize structural advantages at minimal expenses. This paper discusses a methodology for the development of a bulb-tee girder series conforming to LRFD with enhanced structural efficiency relative to the existing girders in Colorado, including performance assessments concerning short- and long-term serviceability and stability. Furthermore, the proposed method provides guidance to other transportation agencies considering new girder systems.

## Background of state-specific bulb-tee girders

Since 1949, when prestressed concrete girders were first used in the United States for the Walnut Lane Bridge in Philadelphia, Pa., significant advancements have been made in design, specifications, and construction. Precast concrete bridge components enhance the quality of construction and save costs. The Federal Highway Administration (FHWA) initiated an effort to explore structurally robust and cost-effective bridge systems in the early 1980s, which led to the development of precast concrete bulb-tee girders. Regarding modern bridge construction, state-specific and non-AASHTO girders are employed by many DOTs. Precast concrete bulb-tee girders are particularly useful for bridge construction where time is considered critical, for example, traffic disruption in an urban environment. Due to the use of high-strength materials, such as concrete and steel strands, bulb-tee girders offer higher load-carrying capacity compared with cast-in-place reinforced concrete tee girders. In addition, pretensioned girders are more economical than post-tensioned girders.<sup>5,6</sup> When planning a highway bridge with precast concrete components, the following items are considered:<sup>7</sup>

- Design of individual girders: Pursuant to design specifications, strength and serviceability limit states in flexure

and shear are checked along with secondary factors such as transfer length, development length, and anchorage. For efficient design, standard sections may be chosen.

- Longitudinal joints: Adjacent girders are connected on-site using shear keys, post-tensioning, or mechanical fasteners at a spacing of 4 to 8 ft (1.2 to 2.4 m). Fatigue may be of interest in avoiding premature joint failure.
- Load distribution among girders: Live-load distribution is a function of joint performance and girder properties (for example, torsional rigidity).
- Limits on length and weight of girders: The weight of individual girders should be limited to 200 kip (890 kN). Shipping and handling can be reasonably facilitated with a girder weight of 155 kip (690 kN) or below and a length of up to 130 ft (40 m).

Various girder types have been proposed, and their configurations are related to span length.<sup>5,8-10</sup>

Extensive endeavors have been made to develop precast concrete bulb-tee girders. Summaries of results from past studies are provided within this section.

Rabbat and Russell<sup>11</sup> compared the structural efficiency and cost-effectiveness of bulb-tee girders with those of conventional I-shapes. The range of investigations involved span lengths from 80 to 160 ft (24 to 49 m) in conjunction with concrete strengths up to 7 ksi (48 MPa). The details of existing girders series for AASHTO, California, Colorado, Illinois, Iowa, Oregon, Pennsylvania, Texas, Washington, and Wisconsin were collected and their performance analyzed. Parameters evaluated were the girders' spacing and length, deck thickness, and concrete strength.

Geren and Tadros<sup>9</sup> reported the developmental history and performance of the NU girder series in Nebraska. Connection methods between the girders were discussed to achieve structural continuity on-site. A numerical analysis was conducted to examine the effects of various parameters, such as girder shape, span length, and strand diameter, on structural behavior under HS25 loading, which considers 90 kip (400 kN) axle loads. A noticeable feature of the NU girders is that the girder webs are reinforced with welded-wire meshes instead of reinforcing bars. By maintaining the constant flange size of the NU girders, precasters can facilitate form fabrication and concrete casting. An implementation plan using the developed girders was presented to construct the Salem West Bridge in Richardson County, Neb.

Meir et al.<sup>2</sup> assessed non-AASHTO bulb-tee girders spanning from 30 to 130 ft (9 to 40 m) at variable girder spacings from 5 to 12 ft (1.5 to 3.7 m) with an emphasis on structural performance and economy. A comparative study with the AASHTO girders was also conducted. The AASHTO I, II, and III girder types were found to be cost-effective

for short spans ranging from 30 to 70 ft (9 to 21 m), whereas Illinois and Kentucky bulb-tee girders showed a better economy for longer spans (70 to 90 ft [21 to 27 m] and 90 to 130 ft [27 to 40 m], respectively), leading to cost savings of about 25%.

Seguirant<sup>5</sup> developed LRFD-based standard bulb-tee girders for the Washington State DOT with consideration for span length, handling, and shipping. The new girders had deeper sections (83 and 95 in. [2108 and 2413 mm] at an increment of 12 in. [304.8 mm]) than the existing Washington State DOT girders to enable longer spans and wider girder spacing. The web widths selected were 6.1 and 7.9 in. (154.9 and 200.7 mm) to avoid the congestion of coarse aggregate in pretensioned and post-tensioned girders, respectively. The top and bottom flanges of the bulb-tee girders had 0.6 in. (15.2 mm) steel strands spaced at 2 in. (50.8 mm) (up to 46 straight and 9 bundled harped-strands in the bottom flange). Harping points for the steel were typically at  $0.4L$ , where  $L$  is the span length, with a maximum slope of 8:1 (horizontal to vertical) for the strands. End blocks (3.3 ft [1 m]) were designed for post-tensioned girders to facilitate jacking operations. On handling and shipping, weight and shapes were taken into account. The method proposed by Mast<sup>12,13</sup> and included in the *PCI Bridge Design Manual*<sup>14</sup> was employed to assess the lateral stability of the developed girders. Site conditions controlled the shipping of the bulb-tee girders with a limitation of 167 to 180 kip (743 to 801 kN) (200 kip [890 kN] may be acceptable).

McMullen and Li<sup>15</sup> studied the feasibility and cost-effectiveness of developing a standardized bridge subset in Colorado. Statistics showed that almost 60% of bridges in Colorado were relevant to standardization of the cross section. By adopting a standardized girder set, cost savings of over \$500,000 per year were expected. When developing standard bridges, four primary items were suggested for consideration: wide applicability, durability, flexibility for construction, and low maintenance.

The span of non-AASHTO bulb-tee girders typically ranges from 70 to 150 ft (21 to 46 m). The use of end blocks is not prevalent for pretensioned girders, though some states (such as Minnesota and Wisconsin) adopt the blocks. Excluding end blocks saves on production costs that would be expended on extra efforts, such as formwork and steel caging. Local precast concrete manufacturers play a crucial role in developing new girder types as the owners and operators of a considerable number of facilities.

## Development of prototype bridge girder configurations

This section details the development of prototype bulb-tee girder configurations. As a starting point, structural efficiency was examined for existing girder series in Colorado and a sensitivity study was conducted in conjunction with optimized dimensions.

**Table 1** shows the BT618 girder series, currently employed in Colorado, and the corresponding sectional properties. The depths of these girders vary from 42 to 84 in. (1067 to 2134 mm) and were designated as CBT42 to CBT84, where CBT stands for concrete bulb tee and the subsequent number represents the depth of the girder.

## Girder development approach

The step-by-step approach taken in the present research to develop prototype bulb-tee girders is as follows:

1. The existing BT618 girder series was assessed for efficiency and performance.
2. Based on optimization techniques, the BT618 sections were revised and trial sections were proposed.
3. A parametric study was conducted to evaluate the structural characteristics of the proposed sections.
4. A prototype section was identified.
5. A comparative assessment was conducted with regard to the efficacy, weight, and geometric properties of the girders.

It was intended to keep the configuration of the BT618 series as much as possible because this series has been used in Colorado for decades and practitioners and precast concrete manufacturers are familiar with it.

The first step was an assessment of structural efficiency, followed by an optimization task to improve the geometric properties. Upon updating the configuration of BT618, trial sections were determined for a parametric study to identify girder dimensions associated with a maximum achievable structural efficiency.

## Sensitivity analysis

**Figure 1** depicts the cross section of the BT618 girders. To examine the effects of dimensional properties on structural efficiency, the section dimensions were represented by seven variables from  $V_1$  to  $V_7$  (Fig. 1). Equations (1) and (2) (proposed by Guyon and Aswad, respectively<sup>11</sup>) are predominantly used in the bridge engineering community when evaluating the efficiency of prestressed concrete girders:<sup>11</sup>

$$\rho = \frac{r^2}{y_t y_b} \quad (1)$$

where

$\rho$  = structural efficiency factor

$r$  = radius of gyration of the girder

$y_t$  = distance from the centroid of the girder section to

**Table 1.** Geometric properties of Colorado bulb-tee girders

Girder	Type	Girder depth $H$ , in.	Cross-sectional area $A$ , in. <sup>2</sup>	Moment of inertia $I$ , in. <sup>4</sup>	Distance from centroid to girder top $Y_t$ , in.	Distance from centroid to girder bottom $Y_b$ , in.	Section modulus for top fiber $S_t$ , in. <sup>3</sup>	Section modulus for bottom fiber $S_b$ , in. <sup>3</sup>	Radius of gyration, $r$
Existing Colorado girder series BT618	CBT42	42	654	153,070	20.85	21.15	7341	7237	15.30
	CBT54	54	738	289,236	27.03	26.97	10,701	10,724	19.80
	CBT63	63	801	425,875	31.64	31.36	13,460	13,580	23.06
	CBT72	72	864	594,937	36.23	35.77	16,419	16,634	26.24
	CBT84	84	948	875,207	42.34	41.66	20,671	21,008	30.38
Prototype	CBT30P	30	616	72,732	15.48	14.52	4695	5009	10.87
	CBT36P	36	652	115,950	18.78	17.22	6174	6733	13.34
	CBT44P	44	700	191,778	23.13	20.87	8291	9189	16.55
	CBT54P	54	760	318,030	28.51	25.49	11,155	12,477	20.46
	CBT63P	63	814	463,897	33.30	29.70	13,931	15,619	23.87
	CBT72P	72	868	642,604	38.05	33.95	16,888	18,928	27.21
	CBT80P	80	916	830,811	42.26	37.74	19,660	22,014	30.12
	CBT88P	88	964	1,048,258	46.44	41.56	22,572	25,223	32.98
Proposed	CBT96P	96	1012	1,296,492	50.60	45.40	25,622	28,557	35.79
	CBT30N	30	678	79,124	15.74	14.26	5027	5549	10.80
	CBT36N	36	720	126,327	19.06	16.94	6628	7457	13.25
	CBT45N	45	783	221,420	21.03	21.03	9237	10,528	16.82
	CBT54N	54	846	347,983	28.83	25.17	12,070	13,825	20.28
	CBT63N	63	909	508,616	33.64	29.36	15,119	17,323	23.66
	CBT72N	72	972	705,906	38.40	33.60	18,383	21,009	26.95
	CBT81N	81	1035	942,430	43.13	37.87	21,851	24,886	30.18
CBT90N	90	1098	1,220,762	47.84	42.16	25,518	28,955	33.35	

Note: CBT = concrete bulb tee; N = new; P = prototype. 1 in. = 25.4 mm; 1 in.<sup>2</sup> = 645.2 mm<sup>2</sup>; 1 in.<sup>3</sup> = 16,390 mm<sup>3</sup>; 1 in.<sup>4</sup> = 416,231 mm<sup>4</sup>.

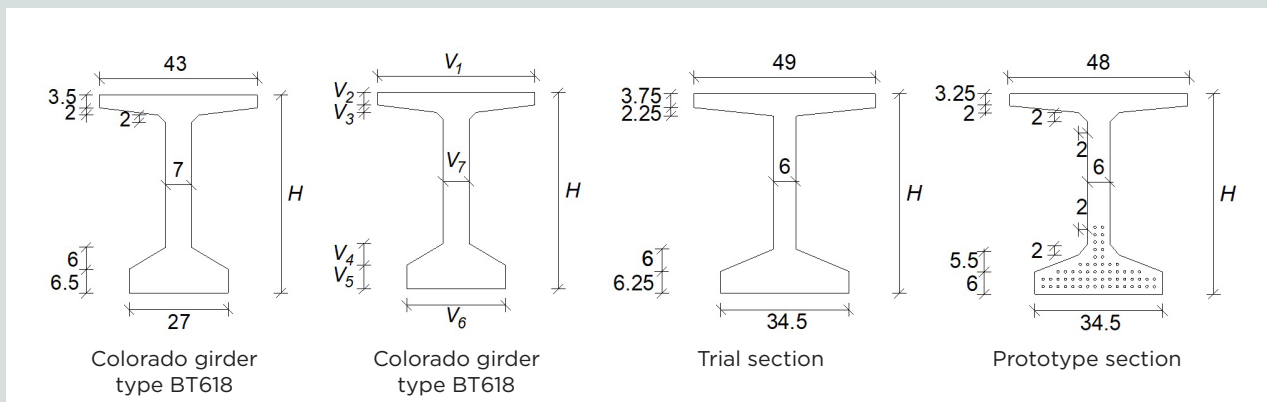


**Figure 1.** Girder dimensions for standard Colorado girder type BT618, parametric study, trial section, and prototype section. Note: All dimensions are in inches.  $V_1$  = upper flange width;  $V_2$  = upper flange thickness;  $V_3$  = upper flange to haunch distance;  $V_4$  = lower flange to haunch distance;  $V_5$  = lower flange thickness;  $V_6$  = lower flange width;  $V_7$  = web thickness. 1 in. = 25.4 mm.

the top fiber

$y_b$  = distance from the centroid of the girder section to the bottom fiber

$$\alpha = \frac{3.46S_b}{Ah} \quad (2)$$

where

$\alpha$  = structural efficiency ratio

$S_b$  = section modulus for the bottom fiber

$A$  = cross-sectional area of the girder

$H$  = depth of the girder

The dimensions of BT618 at a depth of 54 in. (1372 mm) (CBT54) were set as the default, and variable values from  $V_1$  to  $V_7$  were input into Eq. (1) and (2), shown in **Fig. A.1**. (For appendix figures, go to <https://www.pci.org/2020May-Appx.>) With an increase in the upper flange width  $V_1$  from 35 to 51 in. (889 to 1295 mm) (**Fig. A.1**), the efficiency factor  $\rho$  increased from 0.52 to 0.55; however, the efficiency ratio  $\alpha$  decreased from 0.94 to 0.91. This is ascribed to the fact that the denominator of the efficiency ratio (which is the section's cross-sectional area) responded more sensitively as the upper flange of the girder was increased compared with other components of the efficiency factor. Similar observations were made for upper flange thickness  $V_2$ , upper flange to haunch distance  $V_3$ , lower flange to haunch distance  $V_4$ , lower flange thickness  $V_5$ , and lower flange width  $V_6$  (**Fig. A.1**). The web thickness  $V_7$  exhibited an analogous propensity for the variation between the efficiency factor  $\rho$  and efficiency ratio  $\alpha$  (**Fig. 3**), because the increment of the  $r^2$  term in Eq. (1) was proportional to that of the  $S_b/AH$  term in Eq. (2) without markedly changing the  $y_t y_b$  term of Eq. (1). It was thus concluded that these two efficiency approaches cannot be used simultaneously, and Eq. (1) was chosen for the present study. The reason is that Eq. (1) does not depend on an empirical constant, unlike of Eq. (2). This is supported by Seguirant,<sup>5</sup> who stated that the Guyon factor (Eq. [1]) was better accepted than the Aswad ratio (Eq. [2]) for the evaluation of girder efficiency.

## Optimization

The girder dimensions  $V_1$  to  $V_7$  (**Fig. 1**) were optimized to generate the maximum efficiency factor of  $\rho = 0.58$ , which was the highest achievable value according to preliminary calculations. Because seven variables are not likely to be solved simultaneously, each variable was solved one by one. For instance, when determining an optimized value of upper flange width  $V_1$  for a certain girder depth, all other variables were set to the default dimensions of BT618; afterward, the optimized  $V_1$  value was used to determine an optimized value of upper flange thickness  $V_2$  along with other variables: upper flange to haunch distance  $V_3$ , lower flange to haunch distance  $V_4$ , lower flange thickness  $V_5$ , lower flange

width  $V_6$ , and web thickness  $V_7$ . This sequential approach was iterated until the web thickness  $V_7$  was determined. For implementation, an optimization algorithm called the generalized reduced gradient method was employed.<sup>16</sup> **Figure A.2** summarizes the variation of the optimized variables with girder depth. A general trend was that the values of the individual variables rose as the girder depth was increased to maintain the ratio between the radius of gyration term  $r^2$  and the product of distance from the centroid of the girder section to the top fiber  $y_t$  and distance from the centroid of the girder section to the bottom fiber  $y_b$  in Eq. (1). To propose representative values for a girder section, the average values of each variable were taken (**Fig. A.2**). **Figure 1** shows the optimized section of a trial girder. The bottom flange of the trial girder was widened from 30 to 34.5 in. (762 to 876.3 mm) to accommodate more steel strands (16 strands in a row at a spacing of 2 in. [50.8 mm]), which is beneficial from a load-carrying-capacity perspective. This adjusted trial section was used for a parametric study to finalize the dimensions of a prototype bulb-tee girder section. **Figure A.3** exhibits the efficiency factors associated with a girder depth from H30 (30 in. [762 mm]) to H96 (96 in. [2438 mm]) alongside the dimensional variables  $V_1$  to  $V_7$  of the trial section. After careful examinations of the results to achieve the previously mentioned target efficiency factor of  $\rho = 0.58$ , specific dimensions were selected and a prototype girder section was developed (**Fig. 1**).

## Composite section

The theoretical performance of various girder configurations was evaluated using a benchmark bridge superstructure with a reinforced concrete deck of 32 ft (9.8 m) wide and 10 in. [254 mm] thick supported by seven girders at a typical spacing of 55 in. (1397 mm) (**Fig. 2**). The bridge model was simply supported and without skew.

## Bridge modeling

A bridge design and analysis software was used with an assumption of full composite action between the constituents of the superstructure. All modeling details were in conformance with the AASHTO LRFD specifications.<sup>4</sup> The design compressive strength of concrete was  $f'_c = 5$  ksi (34 MPa) for the deck and 8 ksi (55 MPa) for the girders (recommended minimum according to Russell et al.<sup>17</sup>). The initial compressive strength of the prestressed concrete girders was taken as  $f'_{ci} = 6.4$  ksi (44 MPa) (80% of  $f'_c$ ). The prestressing strands had a diameter of 0.6 in. (15.2 mm) at an ultimate strength of  $f_{pu} = 270$  ksi (1860 MPa). The prestressing level applied was  $f_{pj} = 75\%f_{pu}$ , and short- and long-term losses were estimated ( $f_{pe} = 61\%f_{pu}$ ), where  $f_{pj}$  and  $f_{pe}$  were the jacking and effective stresses, respectively.

## Parametric study

Before the determination of a proposed girder section, the following parametric investigations were conducted to evaluate

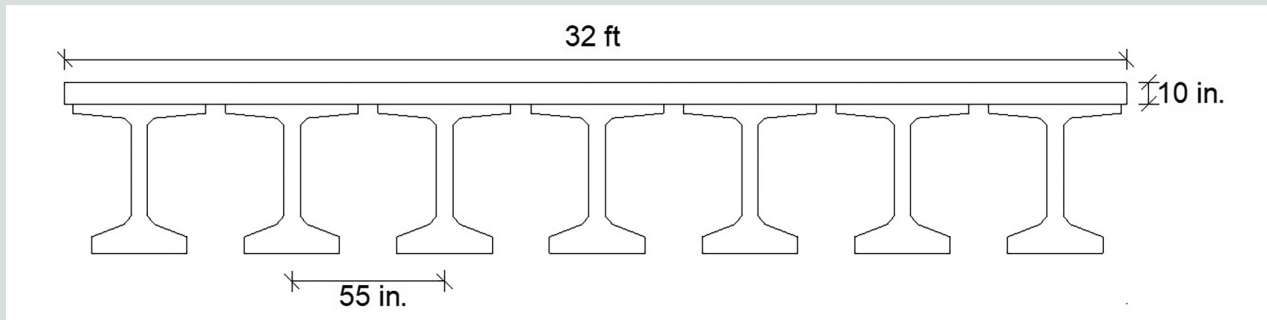


**Figure 2.** Details of a benchmark bridge. Note: Not to scale. 1 in. = 25.4 mm; 1 ft = 0.305 m.

the implications of material and geometric properties on the performance of the prototype bulb-tee girders.

#### Effects of variable web thickness on sectional properties

**Figure A.4** plots the sectional responses of the prototype girder series with a variable web thickness from 6 to 8 in. (152.4 to 203.2 mm). The recommended minimum compressive strength of  $f'_c = 8$  ksi (55 MPa) was used for all cases. As the girder width increased, the efficiency factor dwindled (Fig. A.4). This is attributed to a reduction in the radius of gyration of the section ( $r^2$  in Eq. [1]) with an increase in the web thickness. For example, the efficiency factors of CBT54P (Table 1) with web thicknesses of 6 and 8 in. decreased 6.9% (from  $\rho = 0.58$  to 0.54) when the  $r^2$  term was altered by 6.2% (from  $r^2 = 419$  to 393). The girder weight increased linearly with the depth, regardless of web thickness (Fig. 7). The girder section with an 8 in. web thickness was up to 16.2% heavier than that with a 6 in. thickness (1.05 and 1.22 kip/ft [15.3 and 17.8 kN/m] for CBT96P with 6 and 8 in. web thicknesses, respectively). The thickness of the girder web marginally influenced the section moduli ( $S_t$  and  $S_b$  in Fig. A.4) up to a girder depth of 44 in. (1117.6 mm), after which bifurcations were noticed. The top section modulus  $S_t$  was more susceptible to the girder depth than the bottom section modulus  $S_b$ , owing to the location of the neutral axis that shifted upward with the increased girder depth (that is, the variation rate of  $y_t$  was greater than the rate of  $y_b$ , where  $y_t$  and  $y_b$  are the distances from the neutral axis to the top and bottom fibers of the section, respectively).

#### Effects of variable web thickness on serviceability

**Figures A.5** and **A.6** show the service performance of the girders for stress and deflection, respectively. The sign convention adopted was as follows: positive and negative stresses indicate compressive and tensile, respectively, and downward deflections are positive. The girder-top stresses at release were within the limit of 0.2 ksi (1.4 MPa) in tension (Fig. A.5). The variation of these stresses was insignificant (that is, the web thickness was not a major factor influencing girder stresses). Due to the relatively narrow bottom flange (Fig. 1), the bottom stresses of the girders were clustered and close to the stress limit of 4.2 ksi (29 MPa) in compression. These trends were maintained in the Service I and III examinations conforming to the *AASHTO LRFD Bridge Design Specifications*<sup>3</sup>

(Fig. A.5), and the stress values were within the limits in all cases. This indicates that all of the web thicknesses considered were usable without a problem; in other words, the stress limits should not be a controlling factor when the prototype girders are used to propose an alternative girder section. **Figure A.6** shows the implications of the web thickness on girder deflections. Similar to the case of the stress assessment, no marked influence was noticed. Although their moments of inertia were dissimilar, some girder deflections revealed minimal differences, such as 72 in. (1828.8 mm) compared with 80 in. (2032 mm) and 88 in. (2235.2 mm) compared with 96 in. (2438.4 mm). These minimal differences were attributed to the different span lengths of these girders, which will be detailed in the “Performance Evaluation” section.

### Proposal of new bulb-tee girders

The previously developed prototype girder series was adjusted in accordance with the practical guidance of the Colorado DOT. This section provides the configuration of proposed girders and corresponding structural performance.

#### Adjustment to prototype girders

**Figure 3** illustrates the proposed girder section whose configuration was modified from the prototype girder section owing to nonstructural considerations, such as placing reinforcement, convenience of concrete casting, tendon arrangement, clearance, and handling. The top flange dimensions were altered to employ as potential stay-in-place forming. The web thickness was increased to 7 in. (177.8 mm) to facilitate concrete casting, which may be influenced by the congestion of steel bars. The adjustment of the bottom flange was primarily due to the better placement of steel strands in tandem with various other reasons (for example, diaphragms, bird roosting opportunities, and flood debris snagging). The depth of the girder section was revised for a consistent increment at 9 in. (228.6 mm) from the range of 36 to 90 in. (914.4 to 2286 mm) (Table 1).

### Performance evaluation

**Efficiency Figure A.7** compares the efficiency factors for the proposed, prototype, and existing BT618 girder sections.

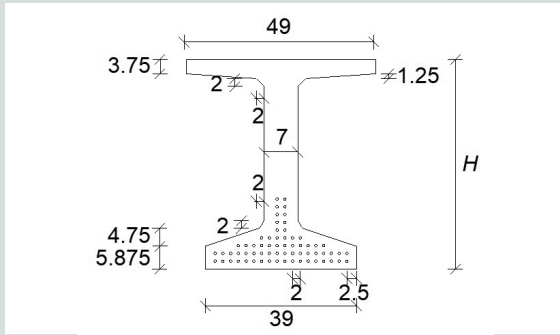


**Figure 3.** Proposed section considering implementation. Note: All dimensions are in inches. 1 in. = 25.4 mm.

The efficiency of the proposed girder series was lower than that of the prototype girder series; however, it was higher than the efficiency of the existing BT618 girders. Because of the increased girder section, the weight of the proposed girders was greater than the weight of the other girders (Fig. A.7). The same trend was observed for the section moduli of the proposed girders, that is, the larger cross-sectional area increased the moment of inertia, thereby raising the section moduli (Fig. A.7). Because of the adjusted geometry, the section capacity of the proposed girders was higher than those of the BT618 and proposed girders (Fig. A.8). The achievable span capacity of the proposed girder series was marginally longer, which required more prestressing strands.

**Serviceability** Related to the span capacity, service requirements for the stress (Fig. A.9) and deflection (Fig. A.10) of the proposed girders were assessed. The stresses of the proposed girders were within the limits of the AASHTO LRFD specifications.<sup>4</sup> The proposed girders exhibited more deflections (Fig. 14) because they had longer spans (Fig. 12). Figures A.11 and A.12 further demonstrate the model analysis results for the camber and deflection of these girders. The average camber of the proposed girders at release was 3.7 in. (93.98 mm), which was analogous to those of the prototype and BT618 girders, 3.8 and 3.9 in. (96.52 and 99.06 mm), respectively). To assess the variation of the cambers with time, material properties and prestress losses at 30 and 60 days were specified in the bridge design and analysis software. There was no marked change in the camber of the proposed girders (Fig. A.11). This illustrates that the camber growth of the girders stabilized within a time frame of 30 to 60 days. It should be noted that the V-shaped camber profiles were attributed to a combination of the prestressing and self-weight effects, leading to nonlinear responses. When a deck was placed at 60 days, the deflections of the girders changed, with reduced upward deflections of 62%, 55%, and 52% for the proposed, prototype, and BT618 girders, respectively (Fig. A.11). Because the material properties and prestressing effects of the girders converged, the 90-day deflections were not dissimilar to the ones plotted in Fig. A.11. Figure A.12 compares the girder deflections with the optional

requirements of the AASHTO LRFD specifications.<sup>4</sup> When the general loading case of  $L/800$  was employed, where  $L$  is the span length, all girder deflections were within the limit (Fig. A.12). In contrast, several cases exceeded the limit for the case of  $L/1000$  (Fig. A.12). The model performance of the girders, however, was not a concern because actual superstructures are stiffer than the simplified bridge models, owing to the presence of secondary elements, such as railings, barriers, and sidewalks.

**Time-dependent deflection** To facilitate the deflection prediction of the proposed girders, time-dependent multipliers were developed by modifying the PCI approach.<sup>18</sup> The following derivation is based on Martin,<sup>19</sup> which was adopted in the *PCI Bridge Design Manual*.<sup>18</sup> The multiplier for the downward component of deflections at erection  $\mu_{de}$  may be expressed as shown in Eq. (3).

$$1 + \mu_{de} = 1 + \left( \frac{\text{loss}_{\text{shrinkage+creep}}}{\text{loss}_{\text{total}}} \right) \frac{E_{ci}}{E_c} \mu_b \quad (3)$$

where

$\text{loss}_{\text{shrinkage+creep}}$  = prestress losses caused by shrinkage plus creep

$\text{loss}_{\text{total}}$  = total prestress loss

$E_{ci}$  = elastic modulus of the concrete at transfer

$E_c$  = elastic modulus of the concrete at 28 days

$\mu_b$  = base factor = 2.0

The ratio of  $E_{ci}$  to  $E_c$  was taken to be 0.85, as recommended by Martin.<sup>19</sup> The prestress loss terms were obtained from the equations of the AASHTO LRFD specifications<sup>4</sup> within a time frame varying from 20 to 60 days. The multiplier for the upward component  $\mu_{pe}$  may be estimated by Eq. (4).

$$1 + \mu_{pe} = 1 + \left( \frac{P_i + P_t}{2P_i} \right) \frac{E_{ci}}{E_c} \mu_b \quad (4)$$

where

$P_i$  = initial (transfer) prestressing force

$P_t$  = prestressing force at time  $t$

In accordance with the AASHTO LRFD specifications,<sup>4</sup> the initial prestressing force  $P_i$  was determined after instantaneous losses, while  $P_t$  was taken as those from 20 to 60 days for consistency. Figure A.13 plots the calculated multipliers for component weight and prestress, respectively. Practitioners can use the following regression equations shown in Eq. (5) and (6).

For deflection due to component weight (downward), the time-dependent multiplier within the application range between 20 and 60 days  $M_w$  is

$$M_w = 1.282t^{0.1081} \quad (5)$$

$t$  = time in days

For deflection due to prestress (upward), the time-dependent multiplier within the application range between 20 and 60 days  $M_p$  is

$$M_p = 1.3075t^{0.0964} \quad (6)$$

**Stability Figure A.14** assesses the stability of the girders per Eq. (7) to (11). The equations were developed by Mast<sup>13</sup> and adopted by the *PCI Bridge Design Manual*<sup>14</sup> and used in the bridge design and analysis software for this analysis.

For hanging:

$$FS_c = FS_f = \frac{1}{\frac{\bar{z}_0}{y_r} + \frac{\theta_i}{\theta_{max}}} \quad (7)$$

where

$FS_c$  = factor of safety for cracking

$FS_f$  = factor of safety for rollover (overturning)

$\bar{z}_0$  = theoretical lateral deflection of the center of gravity of the beam, computed with the full weight applied as a lateral load, measured to the center of gravity of the deflected arc of the beam

$y_r$  = height of the center of gravity of the cambered arc above the roll axis

$\theta_i$  = initial roll angle of the rigid beam =  $e_i/y_r$

$e_i$  = initial lateral eccentricity of the center of gravity with respect to the roll axis

$\theta_{max}$  = tile angle at which cracking begins, based on tension in the top corner equal to the modulus of rupture

During shipping:

$$FS_c = \frac{r(\theta_{max} - \alpha)}{\bar{z}'_0 \theta'_{max} + e_i + y \theta'_{max}} \quad (8)$$

where

$y$  = height of center of gravity of beam above roll axis =  $h_{cg} - h_r$

$h_{cg}$  = height of center of gravity of beam above road

$h_r$  = height of roll center above road

$$FS_f = \frac{r(\theta'_{max} - \alpha)}{\bar{z}'_0 \theta'_{max} + e_i + y \theta'_{max}} \quad (9)$$

where

$\bar{z}'_0$  = theoretical lateral deflection of the center of gravity of the beam but factored to apply to overturning

$\theta'_{max}$  = tile angle at which overturning begins

$$\bar{z}'_0 = \bar{z}_0 (1 + 2.5\theta'_{max}) \quad (10)$$

$$\theta'_{max} = \frac{z_{max} - h_r \alpha}{r + \alpha} \quad (11)$$

where

$z_{max}$  = distance from centerline of vehicle to center of dual tires

The compressive strength of the concrete for hanging and shipping is initial  $f'_{ci}$  and final  $f'_c$ , respectively. As the girder depth increased, the factor of safety regarding cracking and failure for hanging decreased exponentially (Fig. A.14). This trend was maintained when checking on the factor of safety during modeled shipping conditions (Fig. A.14). From a practical viewpoint, care should be exercised when handling a girder with a depth of 72 in. (1828.8 mm) or deeper because the factor of safety drops below 1.5.

## Conclusion

Pursuant to the AASHTO LRFD specifications, a prototype bulb-tee girder series with improved structural efficiency compared with the existing BT618 girder series in Colorado was developed. A sensitivity analysis was conducted to understand the implications of constituent dimensions on efficiency factors followed by optimized girder configurations. Using bridge modeling software, the theoretical performance of the prototype girder section was assessed with a focus on efficiency, sectional properties, serviceability, and achievable span length. Thereafter, a new girder series was proposed (Table 1) following the suggestions of the Colorado DOT. The step-by-step approach taken in this study may be a good reference for those who are interested in developing bulb-tee girders.

## Acknowledgments

The authors gratefully acknowledge financial support from the Colorado Department of Transportation (CDOT). The contents of this paper reflect the views of the authors and do not necessarily reflect the official views of CDOT or any other agencies.

## References

1. Federal Highway Administration Office of Bridges and Structures. "National Bridge Inventory (NBI)." <https://www.fhwa.dot.gov/bridge/nbi.cfm>.

2. Meir, J. V., M. R. Ciccirelli, J. A. Ramirez, and R. H. Lee. 1995. *Alternatives to the Current AASHTO Standard Bridge Sections*. Final report C-36-56GG. West Lafayette, IN: Purdue University.
3. AASHTO (American Association of State Highway and Transportation Officials). 1996. *AASHTO Standard Specifications for Highway Bridges*. 16th ed. Washington, DC: AASHTO.
4. AASHTO. 2016. *AASHTO LRFD Bridge Design Specifications*. 7th ed. and 2016 interim revisions. Washington, DC: AASHTO.
5. Seguirant, S. J. 1998. "New Deep WSDOT Standard Sections Extend Spans of Prestressed Concrete Girders." *PCI Journal* 43 (4): 92–119.
6. Gerges, N., and A. N. Gergess. 2012. "Implication of Increased Live Loads on the Design of Precast Concrete Bridge Girders." *PCI Journal* 57 (4): 64–79.
7. Hieber, D. G., J. M. Wacker, M. O. Eberhard, and J. F. Stanton. 2005. *State-of-the-Art Report on Precast Concrete Systems for Rapid Construction of Bridges*. WA-RD-594.1. Olympia, WA: Washington State Department of Transportation.
8. Lounis, Z., and M. Z. Cohn. 1993. "Optimization of Precast Prestressed Concrete Bridge Girder Systems." *PCI Journal* 38 (4): 60–78.
9. Geren, K. L., and M. K. Tadros. 1994. "The NU Precast/Prestressed Concrete Bridge I-Girder Series." *PCI Journal* 39 (3): 26–39.
10. Caltrans (California Department of Transportation). 2015. *Bridge Design Practice*. 4th ed. Sacramento, CA: Caltrans.
11. Rabbat, B. G., and H. G. Russell. 1982. "Optimized Sections for Precast Prestressed Bridge Girders." *PCI Journal* 27 (4): 88–104.
12. Mast, R. F. 1989. "Lateral Stability of Long Prestressed Concrete Beams—Part 1." *PCI Journal* 34 (1): 34–53.
13. Mast, R. F. 1993. "Lateral Stability of Long Prestressed Concrete Beams—Part 2." *PCI Journal* 38 (1): 70–88.
14. PCI Bridge Design Manual Steering Committee. 2014. *PCI Bridge Design Manual*. MNL-133. 3rd ed. Chicago, IL: PCI.
15. McMullen, M., and C. Li. 2015. *Feasibility Study of Developing and Creating a Standardized Subset of Bridge Plans*. CDOT-2015-05. Denver, CO: Colorado Department of Transportation.
16. Lasdon, L. S., R. L. Fox, and M. W. Ratner. 1973. *Nonlinear optimization using the Generalized Reduced Gradient method*. Report AD-774723. Office of Naval Research Technical Memorandum 325. Springfield, VA: National Technical Information Service, U. S. Department of Commerce.
17. Russell, H. G., J. S. Volz, and R. N. Bruce. 1997. *Optimized Sections for High-Strength Concrete Bridge Girders*. FHWA-RD-95-180. McLean, VA: Federal Highway Administration.
18. PCI Industry Handbook Committee. 2010. *PCI Design Handbook: Precast and Prestressed Concrete*. MNL-120. 7th ed. Chicago, IL: PCI.
19. Martin, L. D. 1977. "A Rational Method for Estimating Camber and Deflection of Precast Prestressed Members." *PCI Journal* 22 (1): 100–108.

## Notation

- |                          |   |
|--------------------------|---|
| $A$                      | = cross-sectional area of the girder  |
| $e_i$                    | = initial lateral eccentricity of the center of gravity with respect to the roll axis |
| $E_c$                    | = elastic modulus of the concrete at 28 days  |
| $E_{ci}$                 | = elastic modulus of the concrete at transfer   |
| $f_{pe}$                 | = effective stress  |
| $f_{pj}$                 | = jacking stress  |
| $f_{pu}$                 | = ultimate strength of prestressing strands   |
| $f'_c$                   | = strength of concrete  |
| $f'_{ci}$                | = initial strength of the prestressed concrete girder                                 |
| $FS_c$                   | = factor of safety for cracking   |
| $FS_f$                   | = factor of safety for rollover (overturning)   |
| $h_{cg}$                 | = height of center of gravity of beam above road                                      |
| $h_r$                    | = height of roll center above road  |
| $H$                      | = depth of girder   |
| $loss_{shrinkage+creep}$ | = prestress losses caused by shrinkage plus creep                                     |
| $loss_{total}$           | = total prestress loss  |
| $L$                      | = span length   |

$M_p$	= the time-dependent multiplier within the application range between 20 and 60 days for deflection due to prestress (upward)	$\theta_i$	= initial roll angle of the rigid beam
$M_w$	= the time-dependent multiplier within the application range between 20 and 60 days for deflection due to component weight (downward)	$\theta_{max}$	= tile angle at which cracking begins based on tension in the top corner equal to the modulus of rupture
$P_i$	= initial (transfer) prestressing force	$\theta'_{max}$	= tile angle at which overturning begins
$P_t$	= prestressing force at time $t$	$\mu_b$	= base factor
$r$	= radius of gyration of the girder	$\mu_{de}$	= downward component of deflections at erection
$S_b$	= section modulus for the bottom fiber	$\mu_{pe}$	= upward component of deflections
$S_t$	= top section modulus	$\rho$	= structural efficiency factor
$t$	= time		
$V_1$	= upper flange width		
$V_2$	= upper flange thickness		
$V_3$	= upper flange to haunch distance		
$V_4$	= lower flange to haunch distance		
$V_5$	= lower flange thickness		
$V_6$	= lower flange width		
$V_7$	= web thickness		
$y$	= height of center of gravity of beam above roll axis		
$y_b$	= distance from the centroid of the girder section to the bottom fiber		
$y_r$	= height of the center of gravity of the cambered arc above the roll axis		
$y_t$	= distance from the centroid of the girder section to the top fiber		
$z_{max}$	= distance from centerline of vehicle to center of dual tires		
$\bar{z}_0$	= theoretical lateral deflection of the center of gravity of the beam		
$\bar{z}'_0$	= theoretical lateral deflection of the center of gravity of the beam but factored to apply to overturning		
$\alpha$	= structural efficiency ratio		
$\alpha_s$	= superelevation angle or tilt angle of supports in radians		

## About the authors



Yail J. Kim, PhD, PEng, FACI, is president of the Bridge Engineering Institute, An International Technical Society, and a professor in the Department of Civil Engineering at the University of Colorado–Denver. His research interests encompass advanced

composite materials for rehabilitation, structural informatics, complex systems, and science-based structural engineering, including statistical, interfacial, and quantum physics.



Thushara Siriwardanage is a PhD student in the Department of Civil Engineering at the University of Colorado–Denver. He is interested in structural behavior subjected to aggressive environments and prestressed concrete bridges.

## Abstract

This paper presents a methodology to develop prestressed concrete bulb-tee girders based on load- and resistance-factor design, particularly for addressing the immediate needs of Colorado. A historical overview of bulb-tee girders in the United States is provided along with important considerations and detailed endeavors, which give the reason for employing state-specific girders. The structural efficiency of the BT618 girders currently used in Colorado is examined and, through an optimization technique, prototype girder sections are established for parametric investigations. With the web thickness varying from 6 to 8 in. (152.4 to 203.2 mm), physical properties of the prototype girders alter, leading to a change in serviceability. Following practical suggestions from the Colorado Department of Transportation, the prototype girders were adjusted to a proposed girder series. Using bridge modeling software, the theoretical performance of the proposed girders was comparatively evaluated against the prototype and BT618 girders with an emphasis on efficiency, stress, achievable span length, time-dependent camber and deflection, and stability for hanging and during shipping.

## Keywords

Bulb-tee girder, development, load- and resistance-factor design, LRFD.

## Review policy

This paper was reviewed in accordance with the Precast/Prestressed Concrete Institute's peer-review process.

## Reader comments

Please address any reader comments to *PCI Journal* editor-in-chief Tom Klemens at [tklemens@pci.org](mailto:tklemens@pci.org) or Precast/Prestressed Concrete Institute, c/o *PCI Journal*, 8770 W. Bryn Mawr Ave., Suite 1150, Chicago, IL 60631. [f](#)